BreastCare

Original Article

Breast Care 2017;12:224–229
DOI: 10.1159/000475745

Published online: August 29, 2017

Dynamic Contrast-Enhanced Magnetic Resonance Imaging in the Assessment of Inflammatory Breast Cancer Prior to and After Neoadjuvant Treatment

Dominique J.P. van Uden[a] J. Hans W. de Wilt[a] Carla Meeuwis[b]
Charlotte F.J.M. Blanken-Peeters[c] Ritse M. Mann[d]

[a] Department of Surgical Oncology, Radboud University Medical Center Nijmegen, Nijmegen, The Netherlands;
[b] Department of Radiology, Rijnstate Hospital, Arnhem, The Netherlands;
[c] Department of Surgery, Rijnstate Hospital, Arnhem, The Netherlands;
[d] Department of Radiology, University Medical Center St. Radboud, Nijmegen, The Netherlands

Keywords

Magnetic resonance imaging · Inflammatory breast cancer · Neoadjuvant treatment

Summary

Background: The aim of this study was to describe the dynamic contrast-enhanced magnetic resonance imaging (DCE-MRI) features of inflammatory breast cancer (IBC) and to assess the value of DCE-MRI for the prediction of pathological complete response (pCR). **Methods:** Image analysis was performed in 15 patients with IBC (cT4d) and 12 patients with non-IBC (cT2), and included the assessment of BIRADS characteristics, skin alterations, enhancement characteristics, and changes post chemotherapy. Sensitivity and specificity of DCE-MRI for the presence of residual disease were obtained. Pearson's correlation coefficients were calculated comparing the (preoperative) tumor size with the histological size. **Results:** Skin thickening/enhancement (80%) and non-mass-like enhancement (66.7%) occurred more often in IBC (16.7 vs. 8.3% in non-IBC). In 2 of 3 cases of IBC, pCR was correctly predicted (sensitivity 92%, specificity 67%), compared to 3 of 5 cases in non-IBC (sensitivity 86%, specificity 40%). Lower peak enhancement might be associated with a higher likelihood of pCR in IBC. No other parameters predicted eventual pCR. In IBC, no correlation between preoperative tumor size and histological size was found ($r = 0.22$, $p = 0.50$), whereas in non-IBC, size estimations were more accurate ($r = 0.75$, $p = 0.03$). **Conclusion:** IBC is characterized on MRI by skin changes and non-mass-like enhancement. Radiological complete response seems indicative of pCR in IBC and non-IBC. Size estimation of residual disease in IBC appears to be inaccurate.

© 2017 S. Karger GmbH, Freiburg

Introduction

Inflammatory breast cancer (IBC) is a rare subtype of locally advanced breast cancer, only accounting for approximately 1% of all breast cancers [1]. According to the TNM classification, IBC is classified as T4d and clinically characterized by diffuse induration of the skin with an erysipeloid edge [2]. Several conditions can mimic the clinical presentation of IBC. Nonpuerperal bacterial mastitis may be confused with IBC, leading to potentially preventable delays in diagnosis and treatment [3]. The skin changes in IBC are caused by tumor emboli within the dermal lymphatics. Although microscopic detection of these emboli is supportive of the diagnosis, it is not required. Furthermore, dermal lymphatic invasion without typical clinical findings is not sufficient for a diagnosis of IBC [4].

The current management of non-metastatic IBC includes a multidisciplinary approach of neoadjuvant chemotherapy (NACT), mastectomy (in the case of axillary lymph node involvement combined with lymph node dissection), and adjuvant locoregional radiotherapy. This multimodal therapeutic approach has significantly improved patient survival in recent years [1, 5]. Nevertheless, IBC still has a poor outcome, with an overall survival of less than 40% at 5 years [1].

KARGER

Fax +49 761 4 52 07 14
Information@Karger.com
www.karger.com

© 2017 S. Karger GmbH, Freiburg

Accessible online at:
www.karger.com/brc

Dominique J.P. van Uden
Department of Surgical Oncology
Radboud University Medical Center Nijmegen
Geert Grootplein Zuid 10, 6525 GA Nijmegen, The Netherlands
djpvanuden@gmail.com

Adequate imaging of the primary tumor, as well as potential metastases, is important for the planning of adequate systemic and locoregional treatment. Magnetic resonance imaging (MRI) is highly sensitive for demonstrating parenchymal breast lesions and skin thickening and is generally used in the diagnostic work-up of patients with IBC [6]. Furthermore, MRI findings can provide a baseline for monitoring response to NACT, and might possibly predict whether or not a pathological complete response (pCR) is achievable or achieved [7]. Also, early identification of non-responders to a particular chemotherapeutic regimen could theoretically lead to a change in treatment. Dynamic contrast enhanced MRI (DCE-MRI) is a valuable tool for the diagnosis, detection, and treatment monitoring in patients with breast cancer since it can define the extent of disease through morphokinetic and pharmacokinetic parameters [8, 9].

The purpose of this study was to compare DCE-MRI imaging features of patients with IBC with those of non-inflammatory breast cancer (non-IBC) patients and to evaluate the predictive possibilities for the assessment of pCR both prior to and after NACT.

Patients and Methods

Patient Selection

Informed consent was waived for this retrospective study. From July 2004 to July 2013, 15 patients with a diagnosis of IBC (T4d) were found to be eligible for this analysis. Patient eligibility criteria included: clinical T4d (cT4d) breast cancer (with histologically proven malignancy) with a baseline breast MRI examination prior to NACT and surgery and a final exam after completing the therapy protocol. From the hospital files, clinicopathological characteristics, radiologic images, and treatment details were extracted. Clinical and pathological TNM stages were determined according to the latest TNM classification of the Union for International Cancer Control (UICC). Exclusion criteria were as follows: patients who only received MRI imaging after NACT and surgery; and non-available MRI images for analysis. A cohort of non-IBC (cT2) patients receiving NACT in order to facilitate wide local excision were selected as a control group and were matched on age at diagnosis with the group of IBC patients.

MRI Examination

All patients had an MRI scan prior to the start of NACT and a second scan after completing the neoadjuvant regimen, before surgery. The availability of MRI scans obtained from patients during chemotherapy, for example halfway through the course of NACT, was variable due to variations in hospital protocols and changes over time. These were therefore excluded from the current evaluation. Patients were all scanned in the prone position in a 1.5 or 3T MRI scanner using a dedicated bilateral breast coil with at least 4 channels (up to 16). The scan protocol also varied over time, but all protocols included a 3-dimensional T1-weighted sequence with a spatial resolution ranging from 1.3 mm isotropic to 1×0.8×0.9 mm. The temporal resolution of this sequence was between 60 and 90 s. The sequence was always performed before contrast administration and repeated 4–6 times thereafter. Contrast (0.1 mmol/kg gadoteric acid, or 0.1 mmol/kg gadopentetate dimeglumine) was administered through an intravenous cannula in the cubital vein after the first acquisition, using a power injector at a speed of 2–2.5 ml/s.

Image Analysis

DynaCAD version 2.0.1.7 (Invivo, Philips, Best, The Netherlands) was used to display acquired images and to extract data. This workstation performs motion correction, and automatically generates subtraction images of all time-points from the T1-weighted pre- and post-contrast acquisitions. Moreover, it automatically generates maximum intensity projections, contrast enhancement versus time curves, and color-coded overlays of contrast kinetics. Using this workstation, R.M., with 11 years of experience in breast MRI, evaluated all lesions on all available MRI scans prior to and after NACT according to the BI-RADS lexicon. The radiologist was blinded to clinicopathological characteristics and treatment results. Lesions were described as either mass or non-mass enhancement, and, if applicable, shape and margin or distribution were described, as well as internal enhancement pattern and shape of the contrast-enhancement versus time curve. Furthermore, the number of large vessels in the affected breast was assessed, and a vessel score was calculated, as well as an assessment of vascular asymmetry according to the method described by Sardanelli et al. [10]. Skin thickening was assessed as absent, focal, or diffuse. Skin enhancement was assessed as absent, focal, regional, or diffuse. Axillary lymph nodes were described as normal, enlarged, or clearly pathological. Lesion size was measured in 3 orthogonal planes. Moreover, the size of each tumor according to response evaluation criteria in solid tumors (RECIST) was assessed as the sum score of the largest diameter of all individual lesions. To obtain a semi-quantitative assessment of enhancement, a volume of interest (VOI) was drawn around each lesion on the subtraction images. This volume of interest is a rectangular box that was drawn in such a fashion that it included the tumor completely, but as little as possible skin, pectoral muscle, and normal enhancing glandular tissue. Subsequently, the volume of the tumor was assessed by calculating the number of voxels within this VOI that reached relative enhancement thresholds of 40 and 100%, respectively. These arbitrary cut-offs were chosen as 100% is commonly used for untreated cancers, whereas several authors have recommended to reduce the threshold for tumors that are treated with NACT to 40% due to the effect of therapy on the leakiness of the vasculature. In these VOI, we also assessed peak enhancement as the value of maximum enhancement in the 1% most enhancing voxels in the volume. Furthermore, we assessed the fraction of voxels exhibiting a type 1, a type 2, and a type 3 curve.

Radiological and Pathological Response Analysis

Specimens were evaluated for pathological treatment response. Radiological response to chemotherapy was classified according to RECIST [11]. pCR to NACT was defined as complete absence of invasive residual disease at the primary tumor site and negative lymph nodes at axillary lymph node dissection or sentinel lymph node biopsy.

Statistical Analysis

The descriptive evaluation of data was performed using the statistical package SPSS for Windows, version 16.0 (IBM Corp., Armonk, NY, USA). The Student's t-test was used to examine significant differences between means of 2 independent samples. Sensitivity and specificity of the post chemotherapy MRI for prediction of the presence of residual disease were assessed. Pearson's correlation coefficients were calculated for the tumor size at MRI scan compared to the size at pathology. A p value of < 0.05 was considered to indicate a significant difference.

Results

Clinicopathological Characteristics

A total of 15 patients with IBC (cT4d) were included in the analysis and compared to 12 patients with non-IBC (cT2) breast cancer. Table 1 displays an overview of clinicopathological characteristics.

All patients in both groups had a preoperatively proven malignancy and underwent NACT (mostly a combination of a taxane with an anthracycline and an alkylating agent) prior to surgery. Mastectomy was performed in all patients with IBC, except for 1 patient with rapidly progressive disease in whom no surgery was

Table 1. Clinicopathological characteristics of all patients with non-inflammatory breast cancer (cT2) versus inflammatory breast cancer (cT4d)

	cT4d	cT2
Age, median (range), years	51.0 (38–67)	44.0 (39–67)
	n (%)	n (%)
Tumor subtype		
Intraductal	15 (100)	12 (80.0)
Lobular	0 (0.0)	0 (0.0)
Other	0 (0.0)	0 (0.0)
Grade		
1	0 (0.0)	0 (0.0)
2	3 (20.0)	1 (8.3)
3	3 (20.0)	3 (25.0)
Unknown	9 (60.0)	8 (66.7)
ER status		
Positive	9 (60.0)	10 (83.3)
Negative	6 (40.0)	2 (16.7)
PR status		
Positive	7 (46.7)	10 (83.3)
Negative	8 (53.3)	2 (16.7)
HER2 status		
Positive	7 (46.7)	2 (16.7)
Negative	7 (46.7)	10 (83.3)
Unknown	1 (6.6)	0 (0.0)
Triple negative	4 (26.6)	2 (16.7)
Distant metastases	4 (26.6)	0 (0.0)

ER = Estrogen receptor; PR = progesterone receptor; HER2 = human epidermal growth factor receptor 2.

Table 2. Magnetic resonance imaging (MRI) features of all patients with non-inflammatory breast cancer (cT2) versus inflammatory breast cancer (cT4d)

	cT4d, n (%)	cT2, n (%)
Number of MRIs		
2	6 (40.0)	3 (25.0)
3	9 (60.0)	9 (75.0)
Skin thickening		
None	1 (6.7)	8 (66.7)
Focal	2 (13.3)	2 (16.7)
Diffuse	12 (80.0)	2 (16.7)
Skin enhancement		
None	1 (6.7)	9 (75.0)
Focal	3 (20.0)	1 (8.3)
Regional	4 (26.7)	2 (16.7)
Diffuse	7 (46.7)	0 (0.0)
Pectoral muscle invasion	2 (13.3)	1 (8.3)
Axillary lymphadenopathy		
Normal	10 (66.7)	9 (75.0)
Enlarged	1 (6.7)	3 (25.0)
Pathological aspects	4 (26.7)	0 (0.0)
Enhancement pattern		
Non-mass enhancement (NME)	10 (66.7)	1 (8.3)
Mass	3 (20.0)	11 (91.6)
NME+Mass	2 (13.3)	0 (8.3)
NME distribution		
Focal	0 (0.0)	0 (0.0)
Segmental	2 (13.3)	1 (8.3)
Regional	3 (20.0)	0 (0.0)
Diffuse	7 (46.7)	0 (0.0)
NME internal enhancement pattern		
Homogenous	0 (0.0)	0 (0.0)
Heterogeneous	11 (73.4)	1 (8.3)
Clumped	1 (6.7)	0 (0.0)
Clustered ring	0 (0.0)	0 (0.0)
Mass margins		
Sharp	0 (0.0)	0 (0.0)
Indistinct	0 (0.0)	5 (41.6)
Spiculated	5 (33.3)	6 (50.0)
Pathological complete response (pCR)	3 (20.0)	5 (41.6)
Radiological complete response (rCR)	2 (13.3)	3 (25.0)
rCR and pCR concordant	2 (66.7)	2 (40.0)

performed after systemic 'NACT'. Radical wide local excision was performed in all cT2 breast cancer patients.

The time interval from presentation at the Department of Surgery to the baseline MRI revealed a median of 7 days (range 0–37 days) in IBC, and 5 days (range -1–17 days) in cT2 breast cancer. A median of 42 days (range 6–77 days) and 26 (range 11–38 days) was observed as interval between the MRI at completion of NACT and surgery for IBC and cT2 breast cancer, respectively.

Patients with IBC were more often diagnosed with estrogen/progesterone receptor-negative tumors (40 vs. 16.7%), and more often with HER2-positive tumors (46.7 vs. 16.7%). At the time of diagnosis, 26.6% of IBC patients already had distant metastases (n = 4; 3 musculoskeletal and 1 liver), and none of the cT2 breast cancer patients had distant metastasis.

DCE-MRI

Table 2 shows imaging characteristics of IBC and cT2 breast cancers prior to NACT. Typically, IBC patients presented with diffuse skin thickening (12/15) and regional or diffuse skin enhancement (11/15). Clearly pathological axillary lymph nodes were found in 4 patients with IBC, compared to none in the non-IBC group. 10 patients with IBC showed non-mass enhancement (10/15), compared to 1 patient in the other group. Furthermore, tumors in the IBC group were evidently larger in size, with more observed vessels in the affected breast.

As shown in table 3, semiquantitative enhancement characteristics were not vastly different between IBC and non-IBC. Peak enhancement was on average 352% in IBC and 317% in non-IBC. A slightly larger fraction of voxels exhibited wash-out characteristics in non-IBC compared to IBC, both at the 100% (10.3 vs. 8%) and 40% (8.1 vs. 5.9%) cut-off values, although this did not reach statistical significance.

Radiological and Pathological Response

For IBC, the average size of the target lesion (RECIST) on the initial pre-NACT DCE-MRI examination was 84.8 ± 33.3 mm and reduced to 28.2 ± 31.4 mm after the completion of NACT (cT2 breast cancer: 26.8 ± 3.9 mm and 14.8 ± 8.7 mm). The aver-

Table 3. Magnetic resonance imaging (MRI) features of 15 patients with inflammatory breast cancer (IBC) and 12 patients with non-inflammatory breast cancer

Parameters	IBC			cT2 breast cancer		
	V^{start}	V^{end}	$V^{end}\_Vstart^{*}$	V^{start}	V^{end}	$V^{end}\_V^{start*}$
RECIST	84.8	45.6	0.54	26.8	14.8	0.55
Lesion size, mm						
Cranial-caudal (CC)	64.3	33.9	0.53	23.7	10.3	0.43
Anterior-posterior (AP)	76.1	34.3	0.45	24.5	12.8	0.52
Left-right (LR)	61.7	32.5	0.53	22.8	11.9	0.52
Number of vessels	4.1	3.3	0.80	2.3	1.4	0.61
Peak enhancement (100% threshold)	352.3	252.6	0.72	316.7	147.3	0.47
Volume (CC 100%)	67.0	18.6	0.28	5.1	0.2	0.04
Volume (CC 40%)	140.3	72.1	0.51	8.0	1.3	0.16
100% curve distribution						
1	41.4	63.8	1.54	31.8	55.0	1.73
2	50.6	33.5	0.66	57.8	36.2	0.63
3	8.0	2.7	0.34	10.3	8.8	0.85
40% curve distribution						
1	56.2	76.2	1.36	49.0	72.0	1.47
2	38.0	21.2	0.56	42.8	20.5	0.48
3	5.9	2.4	0.41	8.1	7.6	0.94

*Percentage of change, V^{end} (MRI parameters after neoadjuvant chemotherapy) relative to V^{start} (MRI parameters prior to neoadjuvant chemotherapy).

Table 4. Magnetic resonance imaging (MRI) features of patients with inflammatory breast cancer (IBC) and non-inflammatory breast cancer with concordant radiological complete response and pathological complete response (pCR)

Parameters	IBC_pCR			IBC_non-pCR			cT2_pCR			cT2_non-pCR		
	V^{start}	V^{end}	$V^{end}\_V^{start*}$	V^{start}	V^{end}	$V^{end}\_V^{start*}$	V^{start}	V^{end}	$V^{end}\_V^{start*}$	V^{start}	V^{end}	$V^{end}\_V^{start*}$
RECIST	99.0	0.0		26.0	0.0		26.9	17.7	0.66	82.6	52.6	0.64
Lesion size, mm												
Cranial-caudal (CC)	57.5	0.0		21.0	0.0		24.2	12.4	0.51	65.3	39.1	0.60
Anterior-posterior (AP)	108.0	0.0		24.0	0.0		24.6	15.3	0.62	71.2	39.5	0.55
Left-right (LR)	60.5	0.0		19.0	0.0		23.5	14.3	0.61	61.9	37.5	0.61
Number of vessels	5.0	3.0	0.60	4.0	0.0		1.9	1.7	0.89	3.9	3.4	0.87
Peak enhancement (100% threshold)	211.0	0.0		297.5	0.0		321.0	176.8	0.55	363.2	274.2	0.75
Volume (CC 100%)	85.1	0.0		4.6	0.0		5.2	0.24	0.05	65.6	20.0	0.30
Volume (CC 40%)	131.1	0.0		7.4	0.0		8.1	1.59	0.20	141.0	77.7	0.55
100 % curve distribution												
1	66.1	0.0		38.8	43.8	1.13	30.3	56.1	1.85	39.5	63.8	1.62
2	33.6	0.0		56.1	50.1	0.89	58.2	34.8	0.60	51.9	33.5	0.65
3	0.3	0.0		5.2	6.1	1.17	11.5	9.1	0.79	8.6	2.7	0.31
40 % curve distribution												
1	76.2	0.0		57.9	72.5	1.25	47.0	71.9	1.53	54.6	76.2	1.40
2	23.7	0.0		37.9	24.8	0.65	43.9	20.1	0.46	39.1	21.2	0.54
3	0.2	0.0		4.2	2.8	0.67	9.0	8.0	0.89	6.3	2.5	0.40

*Percentage of change, V^{end} (MRI parameters after neoadjuvant chemotherapy) relative to V^{start} (MRI parameters prior to neoadjuvant chemotherapy).

age tumor volume of IBC was initially 66.9 cm^3 and reduced to 13.5 cm^3 after the completion of NACT, yielding an average volume decrease of 79.8% after completion of NACT (cT2 breast cancer: 5.1 cm^3 reduced to 0.2 cm^3; average decrease 96%). In all cancers, the fraction of voxels that exhibited continuous enhancement patterns increased relative to the fraction of voxels that exhibited plateau and wash-out curves, both at the 100 and 40% thresholds (table 3).

The average size of the IBC target lesion at pathology was 21.6 mm after completion of NACT (in 3 patients, no tumor was found, and in 2 patients, the pathologist could not reliably measure the size), leading to a decrease of 74.5% compared to the baseline

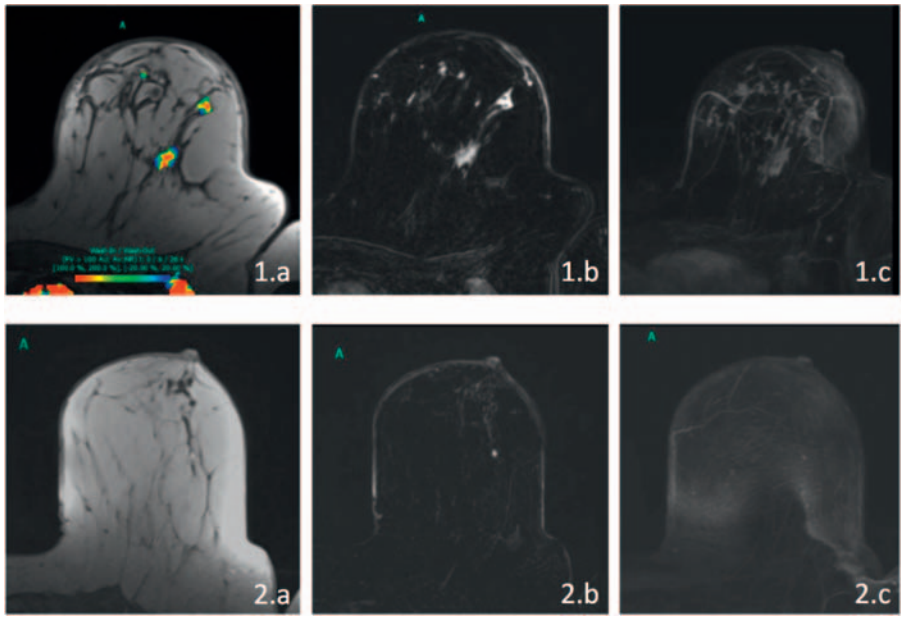

Fig. 1. Dynamic contrast-enhanced magnetic resonance imaging (DCE- MRI) evaluation of a woman with inflammatory breast cancer (IBC) who achieved pathological complete response (pCR). **1.a–c** Pretreatment MRI; **2.a–c** Depiction of the post therapy situation (**a** T1-weighted image with color coding of relative enhancement; **b** subtraction image of the same slice; **c** maximum intensity projection of the affected breast). Prior to therapy, there were multiple regions of non-mass enhancement throughout the left breast. The skin of the entire breast was thickened, and it was regionally (lateral, best seen in 1.b) enhancing. After therapy, the skin changes have normalized, and no residual tumor is apparent.

measurements. The correlation coefficient for the final tumor size between MRI and pathology was 0.22 (p = 0.50) for IBC and 0.75 (p = 0.03) for non-IBC.

A total of 3 (20%) patients with IBC achieved radiological complete response without any detectable lesion in the DCE-MRI study (fig. 1). In 2 patients, also no invasive tumor was found at histopathological evaluation yielding a sensitivity of 92% and a specificity of 67% for the detection of residual disease.

In the cT2 breast cancer group, 5 (42%) patients achieved pCR. In 3 patients, a radiological complete response was found, of which 2 were concordant with the histopathological analysis, yielding a sensitivity of 86% and a specificity of 40% for the detection of residual disease.

When comparing the enhancement characteristics of IBC and non-IBC in which a pCR was achieved to those of the cancers that did not achieve pCR, we observed that IBC that achieved pCR had lower peak enhancement (211 vs. 363%) and a larger fraction of voxels exhibiting type 1 enhancement curves at both thresholds, as is shown in table 4. Morphological descriptors did not differ between groups.

Discussion

In our study, in patients with IBC, skin changes (enhancement and thickening) and non-mass enhancement were the most common imaging features on MRI, as was also found in other studies [12, 13]. While residual size estimation in IBC appears more difficult than in non-IBC, evaluation of the presence of residual disease in IBC after NACT seems at least as accurate as in non-IBC.

IBC is a rare subtype of locally advanced breast cancer with a dismal prognosis [1]. It is a clinical diagnosis made based on the onset of an erythematous and swollen breast in combination with histological proof of invasive breast cancer [14]. Diffuse distribution of parenchymal lesions, and commonly the absence of a discrete mass, impede the diagnostic process [15], and may partly explain the longer work-up times observed for our IBC patients when compared to the non-IBC population. MRI has a key role in the imaging of IBC, since it permits identification of areas susceptible for biopsy, and informs about the actual extent of the disease.

Non-mass-like enhancement was the most common enhancement pattern in patients with IBC. Previous studies suggested that MRI assessment in non-mass lesions after NACT might lead more often to a false-positive diagnosis of pCR. Therefore, MRI for diagnosing pCR in non-mass type IBC should be interpreted with care. However, in our study, the response assessment of pCR in IBC was more reliable than in non-IBC (although not significantly due to limited numbers). The non-mass nature of the lesions might also partly explain the difficulty in assessing the residual tumor size. Further causes include the intrinsic limitations of MRI in detecting small scattered tumors and faintly enhanced residual tumor [7], and the huge distortion of the specimen during histopathological work-up in which the breast is flattened and sectioned before the lesion is measured. Despite these limitations, prediction of response and residual tumor size after NACT seem to be reasonably possible with MRI. Still, earlier separation of these groups might enable the multidisciplinary team to identify non-responders at a time when it is still possible to offer an alternative treatment regimen. Therefore, an evaluation of response using MRI during treatment could provide a relatively sensitive early assessment of chemotherapy efficacy [7], as is commonly advised. However, remarkably, 6 (40%) patients with IBC did not receive an interim MRI assessment, and only the baseline and post-NACT MRI were available. Therefore, in this study, we did not evaluate the interim scans. It might, however, be advisable to perform radiological evaluation with DCE-MRI after the first cycles of NACT, early during treatment, and after completion of NACT, with the aim to distinguish between responders and non-responders.

In our analysis, we did not detect baseline parameters that can be reliably used for the prediction of pCR prior to NACT. However, the observation that patients with IBC and achieving pCR show relatively lower peak enhancement and a larger fraction of voxels with type 1 curves, warrants further research in larger cohorts. In clinical practice, pCR seems to provide information regarding prognosis, but the implications for therapeutic strategies remain unclear, especially in patients with IBC. Selected patients with smaller tumors might be candidates for watchful waiting if a clinical or radiological complete response has been obtained. This has not been incorporated in daily practice, and future research should further elucidate this. Nonetheless, in 2012, a study reported long-term outcome of a monocentric clinical trial combining primary chemotherapy with a schedule of anthracycline-based chemotherapy and an alternating split-course of radiotherapy without surgery in patients with IBC. With a median follow-up of 20 years, local control was achieved in 82% of patients. The 10- and 20-year local relapse rates were 26 and 33%, respectively. The 10- and 20-year overall survival rates were 39 and 19%, respectively. This combined regimen therefore allowed similar long-term local control without the use of surgery [16]. For patients not willing to undergo a surgical intervention, this might be an extra-protocol treatment strategy.

There are several limitations to our study, which have to be addressed. First, our retrospective study included relatively small numbers of patients, and the number of pCR cases was also small. However, the concordance between radiological and histological complete response was encouraging, especially for IBC. Our initial search for potential study candidates revealed more patients than we included in this final analysis. Besides being a rare disease [1], we also observed that MRI analysis was not always done properly (e.g. no baseline MRI or even no MRI before surgery). Clear adherence to the guidelines and performance of pretreatment and preoperative MRI scans should be strictly advised. Further studies on larger patient populations are required to achieve sufficient statistical power.

In conclusion, MRI characteristics of IBC are skin thickening and enhancement, extensive non-mass enhancement with type 3 time-intensity curves, and axillary lymphadenopathy. Although with the small number of subjects in our study a definite conclusion could not be drawn, our results suggest that MRI is overall an appropriate imaging modality in the diagnostic process of patients with suspected IBC. Moreover, it is valuable in the evaluation of IBC tumor response following NACT. However, pretreatment imaging parameters to discriminate patients with an eventual pCR have yet to be determined.

Disclosure Statement

The authors declare that they have no conflict of interest. There was no specific funding for this research.

References

1 Van Uden DJ, Bretveld R, Siesling S, de Wilt JH, Blanken-Peeters CF: Inflammatory breast cancer in the Netherlands; improved survival over the last decades. Breast Cancer Res Treat 2017;162:365–374.
2 Sobin LH, Compton CC: TNM seventh edition: what's new, what's changed. Cancer 2010;116:5336–5339.
3 Peters F, Kießlich A, Pahnke V: Coincidence of nonpuerperal mastitis and noninflammatory breast cancer. Eur J Obstet Gynecol Reprod Biol 2002;105:59–63.
4 Edge S, Byrd DR, Compton CC, Fritz AG, Greene F, Trotti A (eds): AJCC Cancer Staging Manual. New York, NY, Springer, 2009. *www.springer.com/it/book/9780387884400#aboutBook*.
5 Dawood S, Merajver SD, Viens P, Vermeulen PB, Swain SM, Buchholz TA, Dirix LY, Levine PH, Lucci A, Krishnamurthy S, Robertson FM, Woodward WA, Yang WT, Ueno NT, Cristofanilli M: International expert panel on inflammatory breast cancer: consensus statement for standardized diagnosis and treatment. Ann Oncol 2011;22:515–523.
6 Yang WT, Le-Petross HT, Macapinlac H, Carkaci S, Gonzalez-Angulo AM, Dawood S, Resetkova E, Hortobagyi GN, Cristofanilli M: Inflammatory breast cancer: PET/CT, MRI, mammography, and sonography findings. Breast Cancer Res Treat 2008;109:417–426.
7 Chen J-H, Mehta RS, Nalcioglu O, Su M-Y: Inflammatory breast cancer after neoadjuvant chemotherapy: can magnetic resonance imaging precisely diagnose the final pathological response? Ann Surg Oncol 2008;15:3609–3613.
8 Huang W, Li X, Chen Y, Li X, Chang M-C, Oborski MJ, Malyarenko DI, Muzi M, Jajamovich GH, Fedorov A, Tudorica A, Gupta SN, Laymon CM, Marro KI, Dyvorne HA, Miller JV, Barbodiak DP, Chenevert TL, Yankeelov TE, Mountz JM, Kinahan PE, Kikinis R, Taouli B, Fennessy F, Kalpathy-Cramer J: Variations of dynamic contrast-enhanced magnetic resonance imaging in evaluation of breast cancer therapy response: a multicenter data analysis challenge. Transl Oncol 2014;7:153–166.
9 Nadrljanski MM, Milošević ZC, Plešinac-Karapandžic V, Maksimovic R: MRI in the evaluation of breast cancer patient response to neoadjuvant chemotherapy: predictive factors for breast conservative surgery. Diagn Interv Radiol 2013;19:463–470.
10 Sardanelli F, Fausto A, Menicagli L, Esseridou A: Breast vascular mapping obtained with contrast-enhanced MR imaging: implications for cancer diagnosis, treatment, and risk stratification. Eur Radiol 2008;17(suppl):48–51.
11 Nishino M, Jagannathan JP, Ramaiya NH, Van Den Abbeele AD: Revised RECIST guideline version 1.1: what oncologists want to know and what radiologists need to know. Am J Roentgenol 2010;195:281–289.
12 Renz DM, Baltzer PAT, Böttcher J, Thaher F, Gajda M, Camara O, Runnebaum IB, Kaiser WA: Inflammatory breast carcinoma in magnetic resonance imaging. A comparison with locally advanced breast cancer. Acad Radiol 2008;15:209–221.
13 Girardi V, Carbognin G, Camera L, Bonetti F, Manfrin E, Pollini G, Pozzi Mucelli R: Carcinoma infiammatorio della mammella e carcinoma mammario localmente avanzato: possibilit?? Di caratterizzazione mediante l'imaging RM. Radiol Medica 2011;116:71–83.
14 Van Uden DJ, van Laarhoven HW, Westenberg AH, de Wilt JH, Blanken-Peeters CF: Inflammatory breast cancer: an overview. Crit Rev Oncol Hematol 2015;93:116–126.
15 Yang WT: Advances in imaging of inflammatory breast cancer. Cancer 2010;116(suppl):2755–2757.
16 Bourgier C, Pessoa EL, Dunant A, Heymann S, Spielmann M, Uzan C, Mathieu MC, Arriagada R, Marsiglia H: Exclusive alternating chemotherapy and radiotherapy in nonmetastatic inflammatory breast cancer: 20 years of follow-up. Int J Radiat Oncol Biol Phys 2012;82:690–695.